Title
Microstructure of {alpha}-Al Base Matrix/SiC Particulate Composites

Authors
Radmilovic, V.
Thomas, G.
Das, S.K.

Publication Date
1990

LBL-28366
UC-404

Lawrence Berkeley Laboratory
UNIVERSITY OF CALIFORNIA

Materials & Chemical Sciences Division

Microstructure of α–Al Base Matrix/SiC Particulate Composites

V. Radmilovic, G. Thomas, and S.K. Das

January 1990

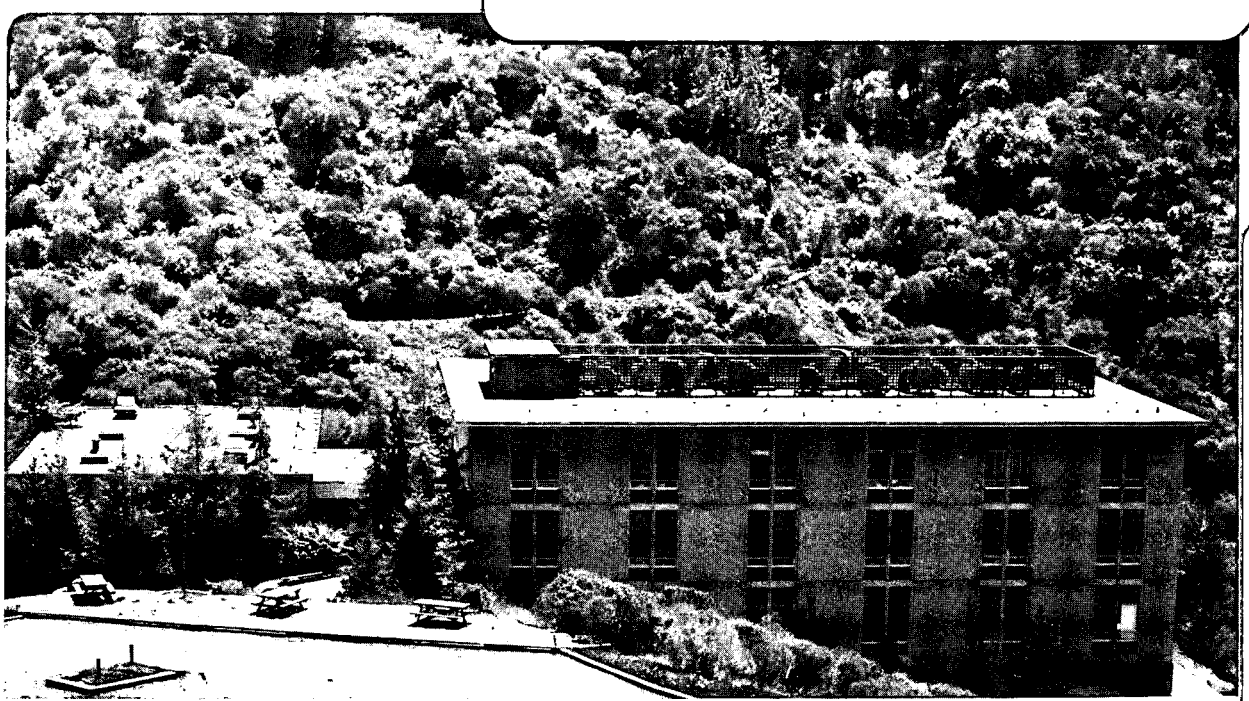

Prepared for the U.S. Department of Energy under Contract Number DE-AC03-76SF00098.

DISCLAIMER

MICROSTRUCTURE OF α-Al BASE MATRIX/SiC PARTICULATE COMPOSITES

V. Radmilovic and G. Thomas
National Center for Electron Microscopy
Lawrence Berkeley Laboratory
University of California
Berkeley, CA 94720

and

S.K. Das
Allied Signal, Metals and Ceramics Laboratory
Morristown, NJ 07960

March 1990

Acknowledgements

It is pleasure to acknowledge the technical assistance of Mr. Chuck Ecker of the National Center for Electron Microscopy. This work was supported by the Director, Office of Energy Research, Office of Basic Energy Sciences, Materials Sciences Division, U.S. Dept. of Energy, under contract DE-AC3-76F00098. The materials were supplied by Allied Signal, Inc. V. Radmilovic also gratefully acknowledges a grant from Allied Signal, Inc., and partial financial support from Research Fund of Serbia (RZNS), Belgrade, Yugoslavia.

MICROSTRUCTURE OF α-Al BASE MATRIX/SiC PARTICULATE COMPOSITES

V. Radmilovic*+, G. Thomas*, and S. K. Das**

*Department of Materials Science and National Center for Electron Microscopy, University of California and Lawrence Berkeley Laboratory Berkeley, CA, 94720

**Allied Signal, Metals and Ceramics Laboratory, Morristown, NJ 07960

Abstract

The microstructures of monolithic Al-Fe-V-Si alloy and α-Al base matrix/SiC particulate composites (MMC) have been characterized by conventional and high resolution transmission electron microscopy, micro-diffraction and X-ray spectroscopy techniques. Silicide particles of average composition $Al_{12}(Fe,V)_4Si$ are present in both of these materials. These particles are unstable under the electron beam at voltages above 200kV, and exhibit radiation induced disordering. SiC particulates present in the MMC structure are predominantly of the hexagonal 6H polytype, but the hexagonal 5H polytype is also observed. A very thin reaction layer is present between the matrix and SiC particles. No segregation of alloying elements such as Fe, V, or Si at the m/SiC interface has been observed. The second phase present at the α-Al/SiC interface seems to be a disordered silicide.

Introduction

Discontinuous reinforced metal matrix composites (MMC) are of great scientific and technological interest and have received much attention in recent years because of their important properties, such as high modulus, high stiffness, and light weight, that make them attractive as a potential substitute for titanium base alloys in high temperature aero-space applications [1-7]. In such composites the nature of interphase interfaces plays an important role in determining the properties and performance, as has been reviewed by Ruhle and Evans [4]. The structure and properties of interfaces in metals, semiconductors, ceramics, and other composites have

---

+ Permanent address: University of Belgrade, Dept. of Metallurgy, Karnegijeva 4, P.O. Box 494, 11001 Belgrade, Yugoslavia.

been extensively studied [8-14]. In many systems such as ceramics, processing methods play a significant role in determining the properties [4, 15-17]. For example, in the case of pure SiC produced by chemical vapor deposition no intergranular boundary layer was observed [17]. However, in many other materials, such as structural and electronic ceramics, amorphous layers are present at interfaces, e.g. as a result of liquid phase sintering. However such layers were not observed by Ruhle and coworkers [14,16] in Nb/Al_2O_3 MMC.

Despite the fact that systematic studies of metal-matrix composites (MMC) started in the early 60's, many very important details such as the atomistic structure and composition of interfaces have remained unclear. Modern sophisticated characterization methods such as high resolution and analytical electron microscopy are indispensable for such studies.

In this research the microstructure of α–Al matrix/SiC composite has been investigated, with particular emphasis on the characterisation of matrix/SiC interfaces (referred to as α-Al/SiC) using high resolution electron optical techniques.

Experimental procedure

The MMC material used in this study was an Al-8.5wt.%Fe-1.3wt.%V-1.7wt.%Si (α–Al) alloy containing 15wt.% of SiC particulates, and a control monolithic unreinforced Al-8.5wt.%Fe-1.3wt.%V-1.7wt.%Si alloy identically processed as the MMC material. The mechanical behavior of the α–Al base composites has been studied in detail by Zedalis et al. [1,2]. Extruded 10mm diameter rods were rolled according to Allied Signal's proprietary practice. The MMC was studied in both the as-extruded and rolled conditions. Hot rolling was performed at 500°C.

For electron microscopy observation discs of 3mm diameter were punched from slices cut by a slow-speed diamond saw, and mechanically polished down to approximately 50μm, and then ion-milled using a cold stage ion-mill unit. In a few cases an alternative method for final thinning has been applied, similar to that used by Dutta and Bourell [3].

Conventional transmission electron microscopy (TEM) has been performed on a Philips 400 electron microscope operating at 100kV. High resolution electron microscopy (HREM) has been performed on a Jeol 200CX and the atomic resolution (ARM) electron microscopes operating at 200 and 800 kV, respectively. Through-focus series of images were taken automatically

in 12 (15)nm increments, starting at the minimum contrast condition. In order to obtain diffraction information from extremely small volumes of the MMC samples nanoprobe diffraction using a 10nm beam diameter has been applied. Laser optical microdiffraction was also used to analyse small details in high resolution images.

Scanning transmission electron microscopy (STEM), energy dispersive X-ray spectroscopy (EDX) and microdiffraction analysis were performed on a JEOL 200CX microscope operating at 200kV. In order to reduce contamination of the thin foil the GATAN cryogenic specimen holder was kept at -160°C. Line scan spectra measured perpendicular to the α-Al/SiC interfaces were obtained by using a 10nm probe size, with a spatial resolution of about 25nm. The error in chemical composition analysis was calibrated with standards, and was within ±1 wt%. Discrete point spectra and microdiffraction were performed by using probe sizes in the range 10 to 30nm.

Results

Monolithic alloy

Fig. 1a shows the typical structure present in the as-extruded monolithic alloy. It consists of $Al_{12}(Fe,V)_4Si$ silicide particles in the α-Al solid solution (matrix). The silicide particle size is in the range between 20 and 100nm. There is a large volume fraction of silicide particles uniformly distributed in the matrix, but there is a tendency to form agglomerates (A in Fig. 1). Fig. 1b shows the selected area diffraction pattern from the region in Fig. 1a. The particles are randomly oriented and do not exhibit any consistent crystallographic orientation relationship to the matrix. The grain size is in the range from 0.5 to 2μm. High resolution electron microscopy (Fig. 2a) and diffraction show that the silicide particles have the b.c.c. structure with lattice parameter a=1.25nm. After approximately 30 sec irradiation under a 800kV beam, the silicide particles become almost completely disordered (Fig. 2b). Under a 200kV electron beam this disordering is slower, taking approximately 45 min to completion. This indicates that the damage is primarily due to knock-on displacements.

General structure of the MMC material

Fig. 3 shows the typical structure in the as-extruded (a) and hot rolled (b) metal matrix composite. The microstructure contains SiC particulates (P) and silicide particles (S) in the α−Al matrix (m). The grain size and the

silicide particle size in the as extruded MMC are approximately the same as those in the as-extruded monolithic alloy, i.e. from 0.5 to 2μm and from 20 to 100nm, respectively. In the hot rolled MMC the silicide particle size is greater and is in the range from 50 to 200nm. The SiC particle sizes in the as-rolled and hot rolled material seem to be the same, and in the range from 0.5 to 5μm.

Structure of SiC

The morphology of SiC particulates is not uniform, but usually shows irregular polygonal geometries. Diffraction pattern analysis and high resolution images show that both allotropes, hexagonal α-SiC (Fig. 4) and cubic β-SiC (Fig. 5) are present in the MMC materials. The hexagonal allotrope has predominantly the 6H polytype structure (Fig. 4), with clearly visible fine micro-twins, as previously observed by Clarke and Thomas [11]. However, the 5H polytype structure, as well as amorphous regions in the hexagonal structure, have also been observed (Fig. 6). This amorphous region is clearly visible at all defocus settings with respect to the Gaussian image plane, and is thus not an artifact of the imaging process.

Structure of the α–Al/SiC interface

Fig. 7 is an example of a the high resolution image of the interface between the hexagonal SiC and the α–Al matrix (m). The interface is usually not sharp nor faceted. It is diffuse, which indicates the existence of an interfacial reaction layer. The interface morphology is different at different SiC particulates and ranges from flat to wavy. EDX analysis (Fig. 8) revealed that no Fe nor V alloying element segregation was detected across the interface with the SiC, i.e. no concentration of these elements that exceeds the amount present in the bulk material or silicide particles has been observed. However, numerous second phase particles at or in the vicinity of the α–Al/SiC interfaces have been resolved (Fig. 3). EDX analysis has also shown that in all cases the cationic elements present at the interface are either Al and Si, or Al, Si, Fe and V. The presence of oxygen in the amount that exceeds oxygen in the surface oxide layer has not been observed. High resolution microscopy of lattice fringes across the α–Al/SiC interface (Fig. 9) shows that the spacing between the unknown planes in the particle present at the interface is 0.236nm, while that of the {0001} planes in the 6H SiC particulate is 0.251nm. Microdiffraction shows (Fig. 10) that the second phase particle at the interface is a silicide, and is the same as that in the control monolithic alloy.

Discussion

Neither the α–Al/SiC nor the silicide/SiC interfaces appear to be coherent as evidenced by image contrast and diffraction analysis for orientation relationships. The distribution of such relationships were found to be random with no common interfacial habit. On the other hand the α–Al/SiC interfaces are planar except when an interface reaction zone is present. However, even in the former case there is no particular crystallographic matching, e.g. $\{0001\}_{SiC} \# \{111\}_{matrix}$. The alloy is thus a noncoherent mechanical mixture. Compared to the simple heterophase Al/SiC, these MCC materials, with the silicides as second phase particles, and Fe, V, and Si as the alloying elements in the α–Al solid solution, are much more complicated. As has been pointed out by Ruhle and Evans [4], even if all the thermodynamic data, for a system that forms interphases, are known, the preferred product phases still cannot be unambiguously determined from the phase diagram, because this problem involves kinetic considerations.

Structure of SiC particulates

The SiC particles are predominantly of the hexagonal 6H polytype structure with microtwins on the 0001 basal planes (Fig. 4). In the images for the defocus conditions adopted, the bright spots represent spaces between the atom columns of silicon and carbon. Each bright spot is surrounded by 6 atom columns. In a few cases it has been found that stacking periodicities of 6 and 5 Si-C layers coexist within the same SiC particulate. The 5H polytype (with c=1.255nm) appears after every 4 unit cells of 6H polytype (axis c=1.507nm). Clarke and Thomas [11] also found stacking sequences having periodicities of 8, 24, 36, 48, and other Si-C layers. These polytypes probably form by faulting involving shear in the basal plane. The partial dislocations so involved can only extend the fault in the plane, i.e. the transforming polytype can not thicken perpendicular to the SiC 0001 basal plane unless new partials are nucleated [15] over the appropriate repeat distances.

Interfaces with SiC

The observation that SiC changes abruptly from the 6H polytype structure in a very narrow region next to the α–Al/SiC interface (Fig. 7b), indicates this is due to a change in composition. Based on the available ternary phase diagram [24] it can be assumed that no solubility of Al, Fe, and V

exists in SiC, and that a very limited amount of Si and C diffusion occurs during extrusion processing into the α–Al matrix. Thus the interfacial reaction layer is very narrow. The driving force for this reaction is such as to lower the free energy of the interface.

For a detailed analysis of the structure and extent of this interface layer, special attention has to be paid by HREM. For example, the interfacial region is susceptible to preferential thinning which could lead to improper interpretation. Figs. 9a and 9b show that at some defocus settings the reaction layer appears to be amorphous. However, a through focus series revealed that no amorphous region exists in this case. Preferential etching near the interface leads to a shadow effect [16], which is similar to that produced by glassy phases [22]. Calculations and crystallographic analysis show that the cross fringes clearly visible in Fig. 9b do not represent a coherent α–Al/SiC interface, as in the case of NiO-ZrO_2 interfaces [19]. In the α–Al/SiC MMC, perfect coherency between SiC particles and matrix is impossible. The misleading apparent coherency from HREM images is caused by overlapped fringes, from interfaces which cannot be atomistically flat.

High resolution image analyses of this transition region is resolved as a region having lattice fringe images of spacing depending on orientation. For example, from the known periodicity of the 6H fringes of spacing 1.5nm in SiC, the transition fringes can be measured quite accurately at 0.236nm. These fringes cannot be uniquely identified in terms of specific phases because their extent is limited, and their dimensional analyses can not be uniquely measured. However, based on the present observations and comparing the data to those available for other compounds such as Al_4SiC_4 [25,26] and silicides [27-29], it is concluded that the interfacial phase at the α–Al/SiC interface is in fact also a silicide phase (or phases). The above conclusions are consistent with the known phases expected for these compositions. The silicide particles in that case serve as a mechanical bond between the matrix and SiC particulates. This bond is facilitated by the hot mechanical processing.

Conclusions

Microstructural and microchemical considerations of an Al-base matrix/SiC particulates composite led to the following conclusions:

1. The MMC material is a mechanical composite of non coherent SiC particulates dispersed within the α–Al matrix and silicide particles.

2. The silicide particles present in the monolithic alloy and the α–Al/SiC metal matrix composite are of the $Al_{12}(Fe,V)_4Si$ type and are similar in size. Radiation induced disordering of these silicide particles occurs by displacement damage, when examined in TEM.

3. The SiC particles present in the MMC material are predominantly of the hexagonal 6H polytype structure, but the hexagonal 5H polytype structure with c axis 1.255nm is also observed. This polytype appears after every 4 unit cells of the 6H polytype structure.

4. A very thin reaction (transition) layer is present between the matrix and the SiC particulates, indicating a limited diffusion reaction exists during extrusion processing. No segregation of alloying elements was observed at the interface with SiC particulates.

5. The transition region is likely to be a disordered silicide partcle.

Acknowledgements

It is pleasure to acknowledge the technical assistance of Mr. Chuck Ecker of the National Center for Electron Microscopy. This work was supported by the Director, Office of Energy Research, Office of Basic Energy Sciences, Materials Sciences Division, U.S. Dept. of Energy, under contract DE-AC3-76F00098. The materials were supplied by Allied Signal, Inc. V. Radmilovic also gratefully acknowledges a grant from Allied Signal, Inc., and partial financial support from Research Fund of Serbia (RZNS), Belgrade, Yugoslavia.

References

1. M.S. Zedalis and D. J. Skinner, Proceed. of "Structural Light Weight Alloys for Aerospace Applications", TMS-AIME, Las Vegas, 1989.
2. M.S. Zedalis, J.M. Peltier, and P.S. Gilman, Proceed. of "Structural Light Weight Alloys for Aerospace Applications", TMS-AIME, Las Vegas, 1989.
3. I. Dutta and D. L. Bourell, Mater. Sci. Eng., **A112**(1989)67.
4. M. Ruhle and A.G. Evans, Mater. Sci. Eng., **A107** (1989)187.
5. S. V. Nair, J. K. Tien, and R. C. Bates, Int. Met. Rev., **30**(1985)275.
6. A. P. Divecha, S. G. Fishman, and S.D. Karmarkan, J. Met., **33**(1981)12.
7. Proceed. of the Symp. on "Interfacial Phenomena in Composites", Newport, 1988, Elsevier Sequoia Publ.
8. N.F. Mott, Proc. R. Soc., **6o**(1948)301.
9. H. Gleiter and B. Chalmers, Prog. Mater. Sci., **16**(1972)1.
10. H. Gleiter and P. Pumphery, Mater. Sci. Eng., **25**(1976)159.
11. D.R. Clarke and G. Thomas, Proceed. Sixth EUREM, Jerusalem, 1976, p.564.
12. M. Ashby, F. Spaen, and S. Williams, Acta Met., **26**(1978)1647.
13. D.R. Clarke, J. Am. Cerm. Soc.,**62**(1979)236.
14. H. Schmid and M. Ruhle, J. Mater. Sci., **19**(1984)615.
15. G. Thomas, "Ceramic Microstructure '86", eds.. J.A. Pask and A.G. Evans, Plenum Press, 1987, p.55.
16. M. Ruhle, M. Backhaus-Ricoult, K. Burger, and W. Mader, in "Ceramic Microstructure'86", J.A. Pask and A.G. Evans, eds., Plenum Press, New York, 1986, p.295.
17. Y. Ishida and H. Ichinose, J. Electron Microscopy, **35**(1986)155.
18. A.K. Vasudevan et al., Mater. Sci. Eng., **A107**(1989)63.
19. V. P. Dravid, C. E. Lyman, and M. R. Notis, and A. Revcolevschi, Ultramicroscopy, **29**(1989)60.
20. V. Radmilovic, G. Thomas and S. Das, to be published.
21. D. R. Clarke, Ultramicroscopy, **29**(1979)33.
22. O.L. Krivanek, T.M. Shaw, and G. Thomas, J. Amer. Ceram. Soc., **62**(1979)585.
23. H. Ichinose, Y. Inomata, and Y. Ishoda, "Ceramic Microstructure'86", eds. J.A. Pask and A.G. Evans, Plenum Press, 1987, p.255.
24. L.L. Oden and R.A. McCune, Met. Trans., **18A**(1987)2005.
25. PDF No. 17-658.
26. PDF No. 35-1072.
27. PDF No. 35-1073.
28. PDF No. 20-30.
29. PDF No. 20-33.

Figure captions

Fig. 1 (a) Bright field image of monolithic Al-Fe-V-Si alloy in as-extruded condition; Note silicide particle agglomerates (A in Fig. 1); (b) Diffraction pattern of the structure in Fig. 1. Note absence of any consistent crystallographic relationship between silicide particles and Al-base matrix.

Fig. 2 HREM images of silicide particle in the 100 orientation; (a) particle exposed approximately 10 seconds to 800kV electron beam; (b) same particle after 45 seconds under 800kV electron beam.

Fig. 3 TEM micrographs of (a) as-extruded and (b) hot-rolled m/SiC composites. Note numerous second phase particles at m/SiC interface, at C in (a), and arrowed in (b); P= SiC particles; S= silicide particles.

Fig. 4 (a) HREM image of hexagonal 6H polytype showing {0001} fringes; b) selected area diffraction pattern of hexagonal SiC particle.

Fig. 5 (a) HREM image of cubic SiC particle showing {111} fringes; (b) selected area diffraction pattern of cubic SiC particle.

Fig. 6 HREM image of hexagonal SiC particle with 6H and 5H polytypes. Note that 5H polytype appears after every 4 unit cells of the 6H polytype structure.

Fig. 7 HREM images of m/SiC interface. Note diffuse nature of interface in (a), and abrupt change of 6H polytype structure in the narrow region next to the interface.

Fig. 8 (a) TEM micrograph corresponding to the region microanalysed in (b); (b) shows composition profile measured in the line scan; a very narrow interfacial layer is evident.

Fig. 9 HREM images of m/SiC interface at different defocus settings; the difference between (a) and (b) is approximately 3.6nm. The spacing of 0001 fringes in the hexagonal 6H SiC is 0.251nm. The spacing between fringes on the matrix side is 0.236nm.

Fig. 10 Nanoprobe diffraction pattern of silicide particle at m/SiC interface in 111 zone axis.

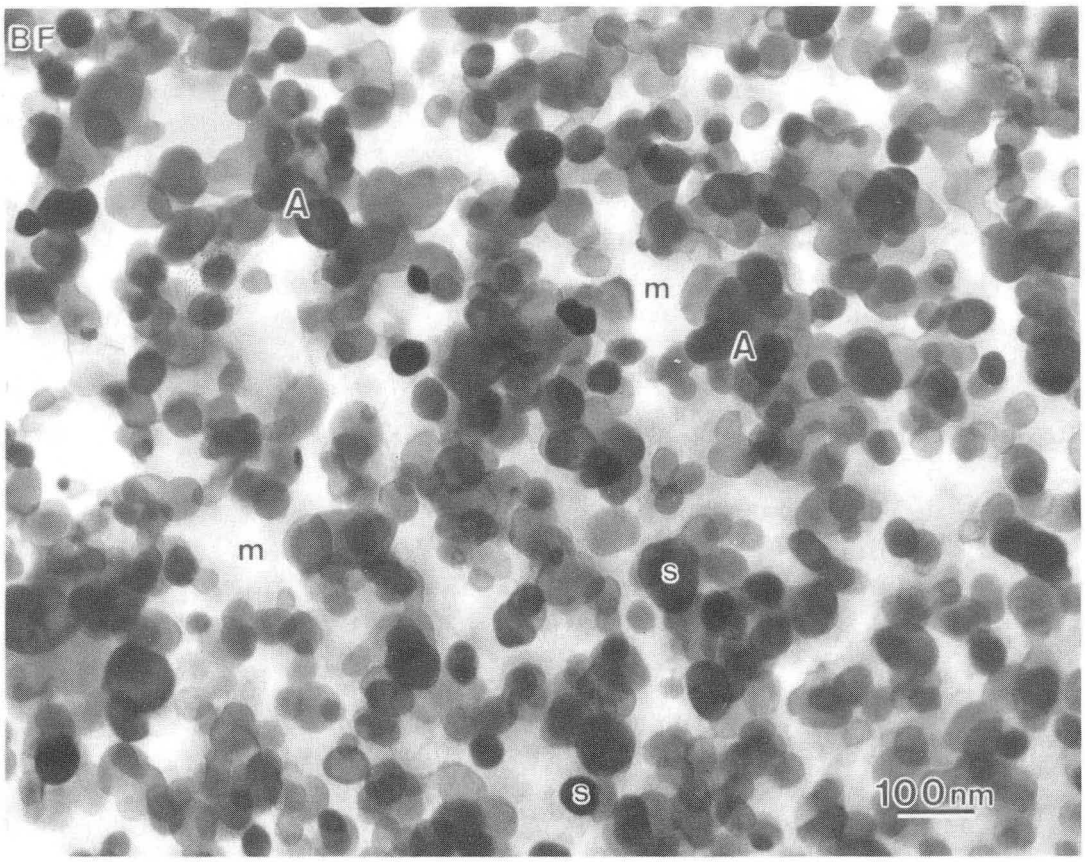

Fig. 1a

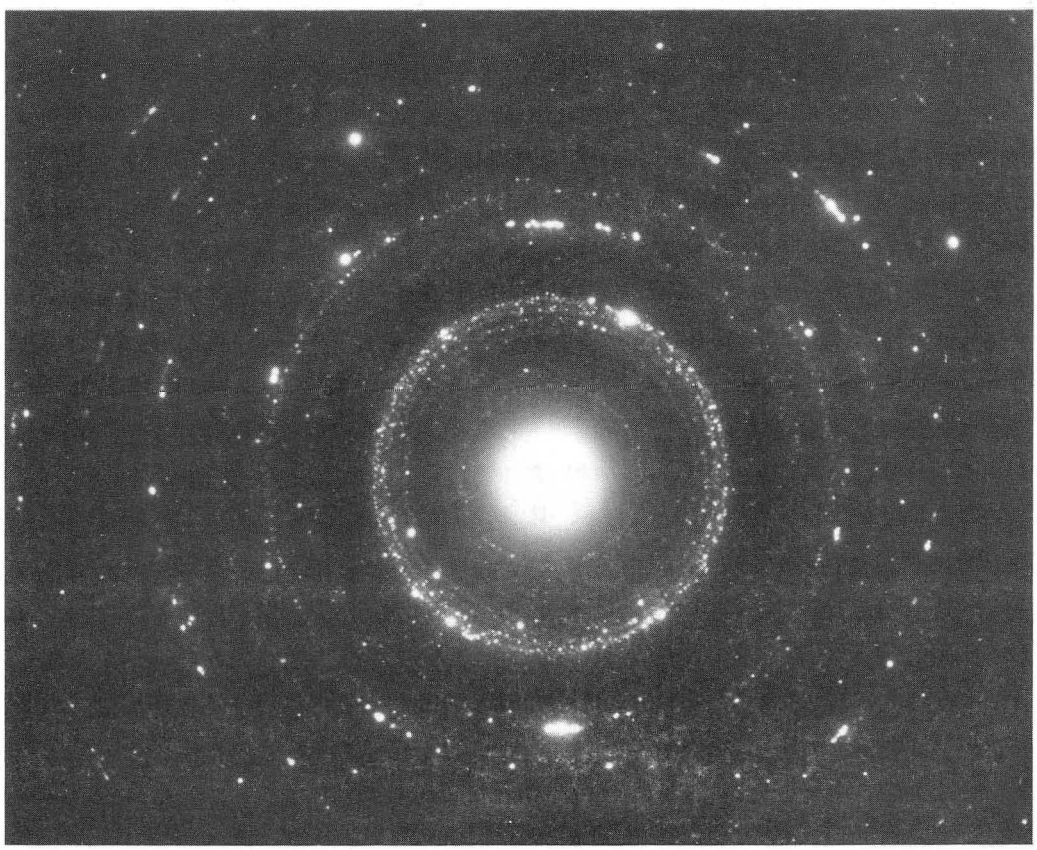

Fig. 1b

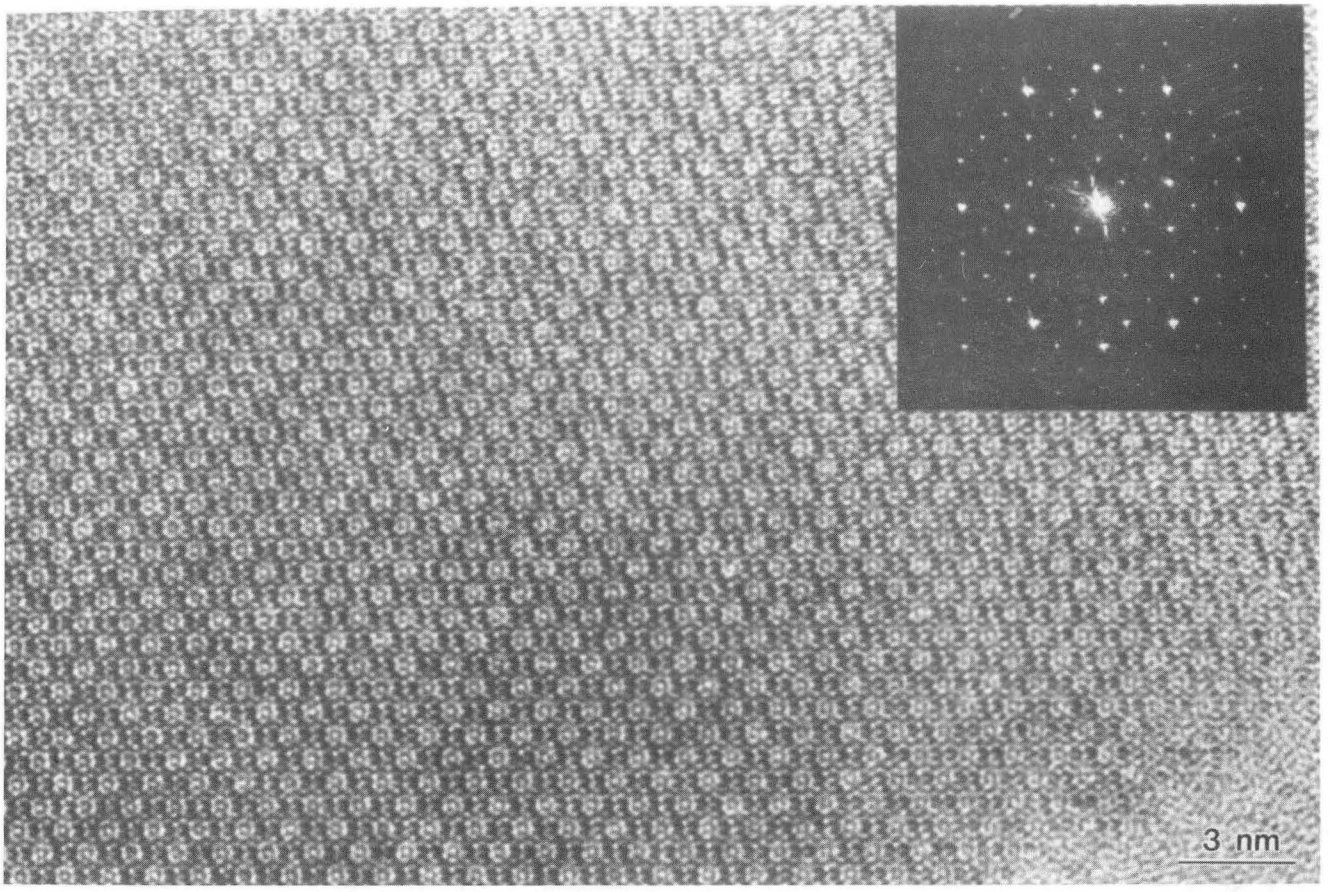

Fig. 2a

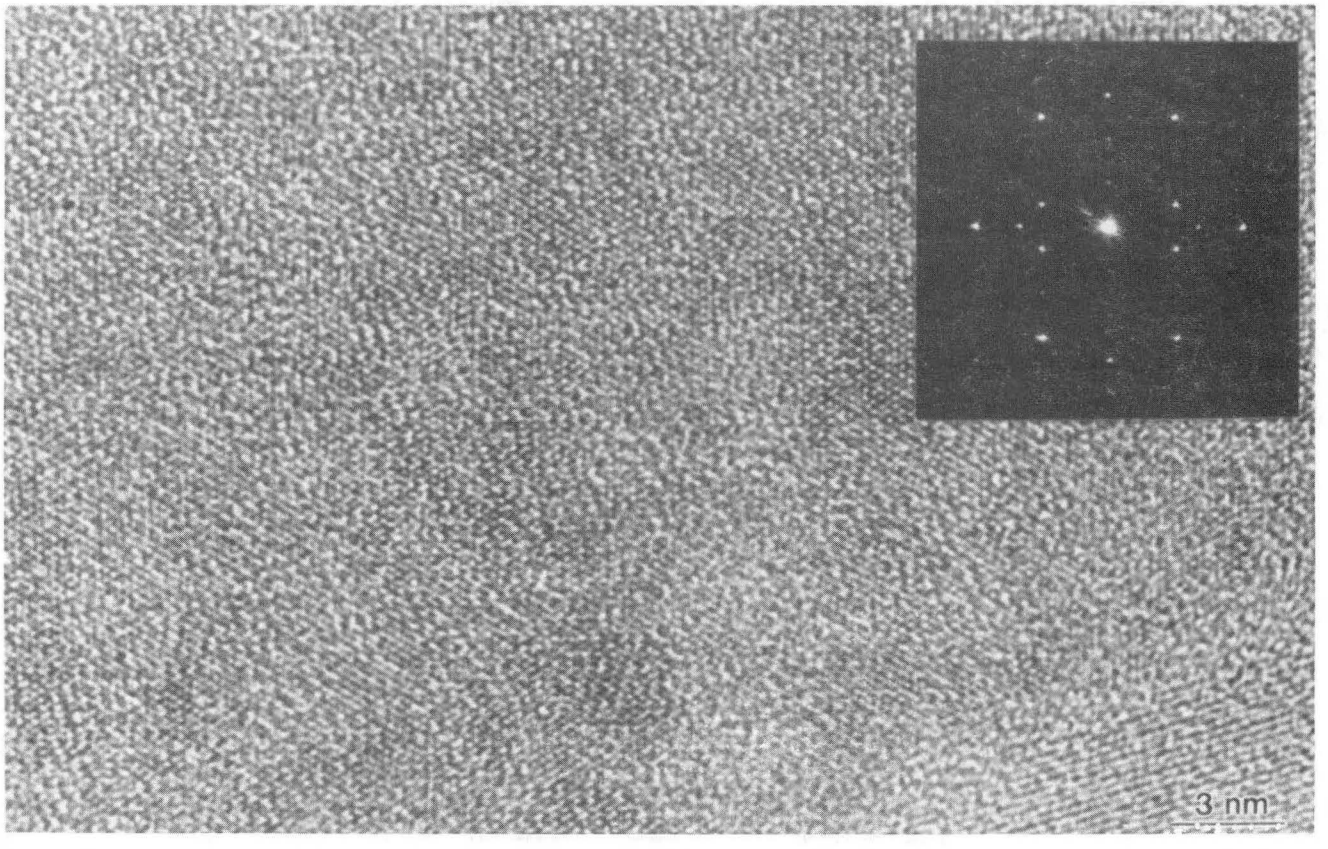

Fig. 2b

XBB 898 7117A

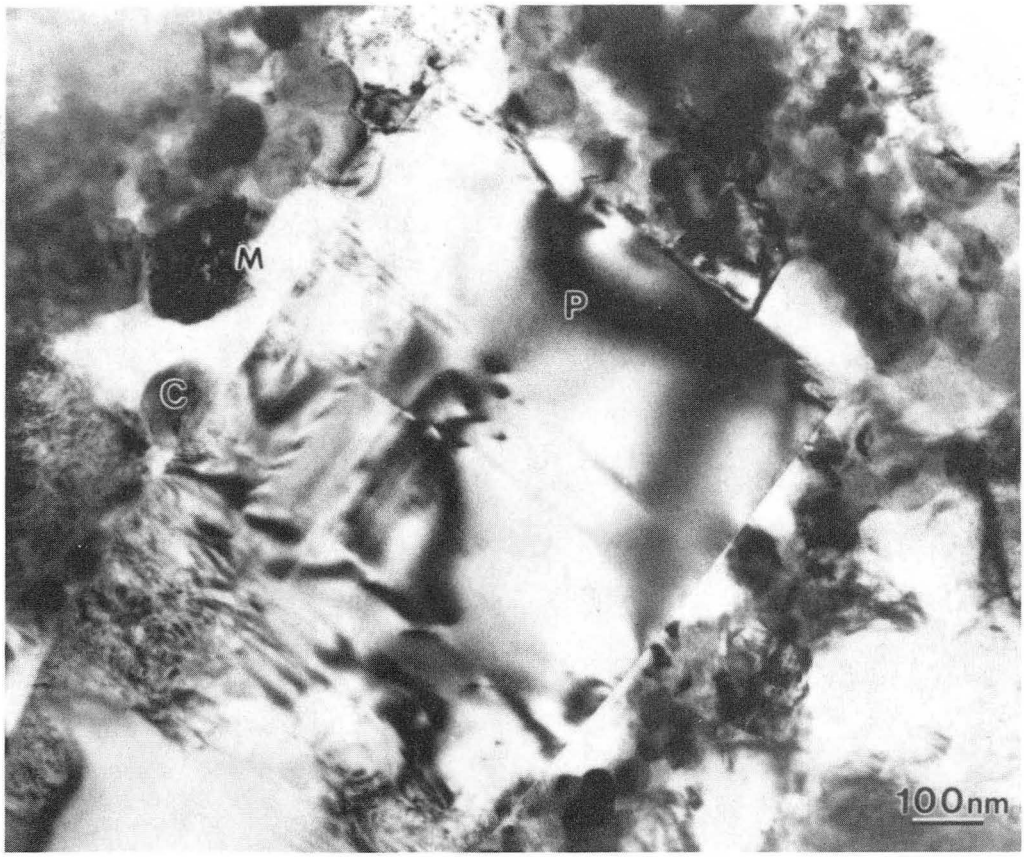

Fig. 3a

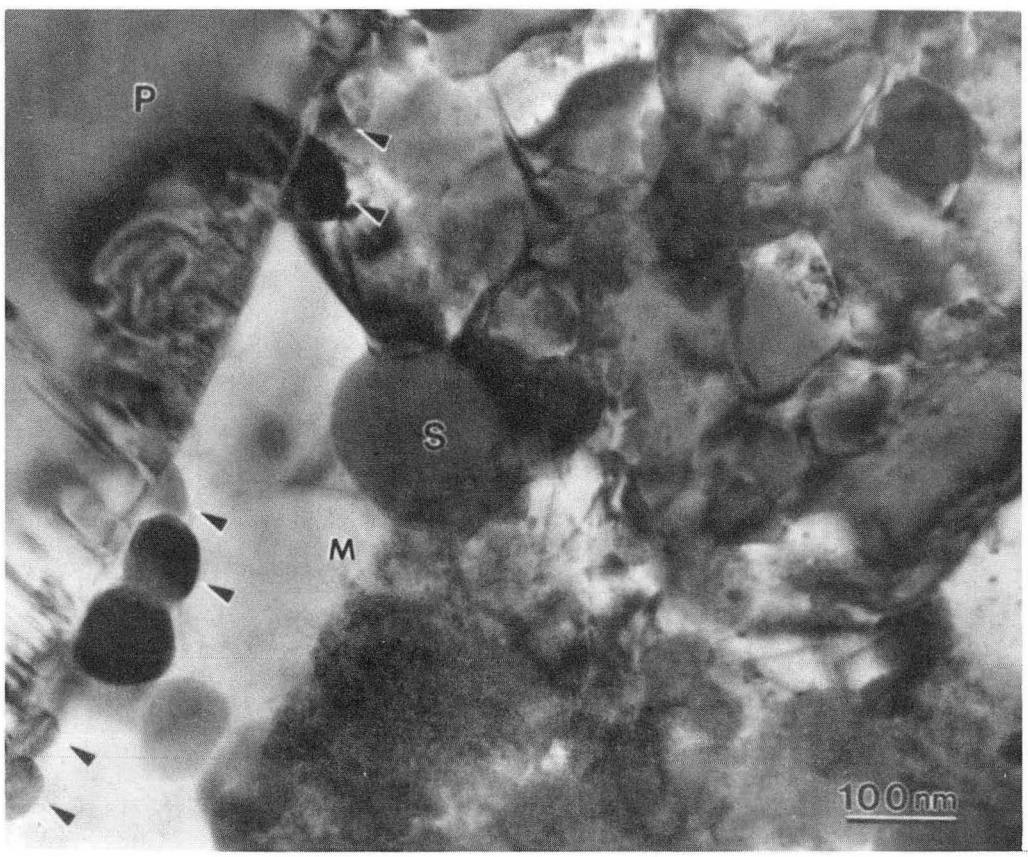

Fig. 3b

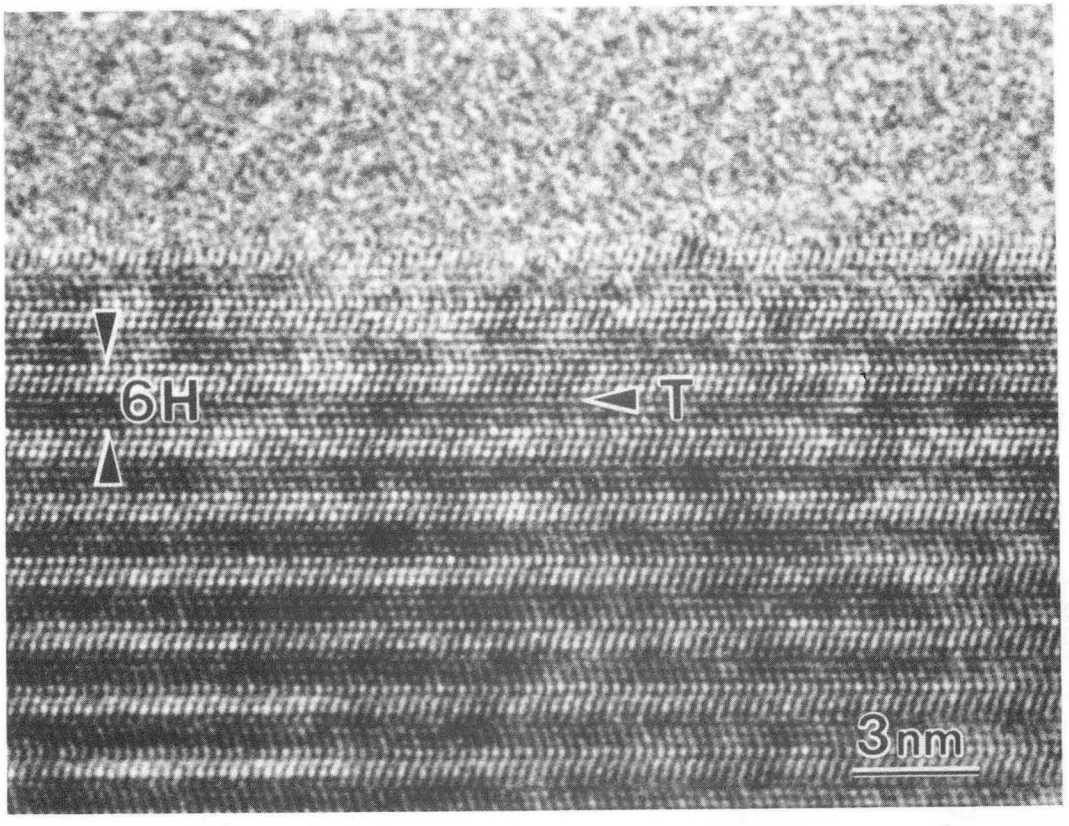

Fig. 4a

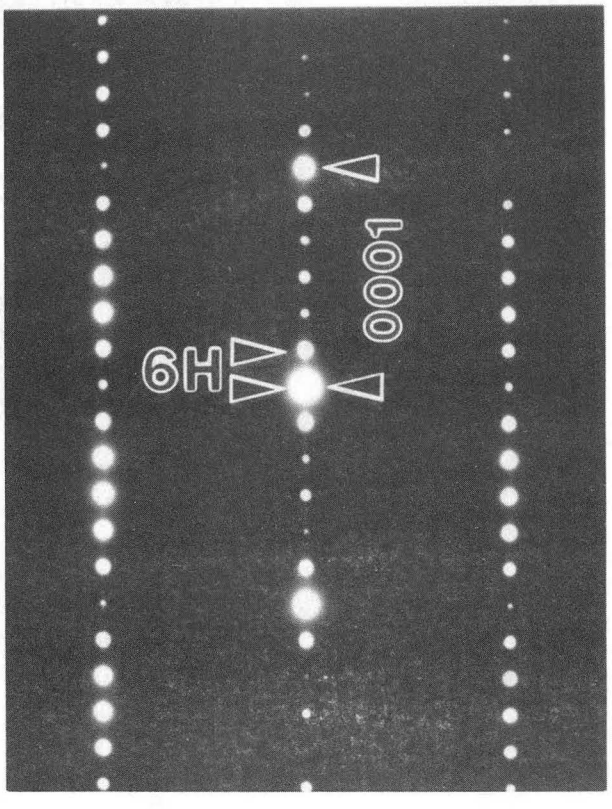

Fig. 4b

XBB 898-7092

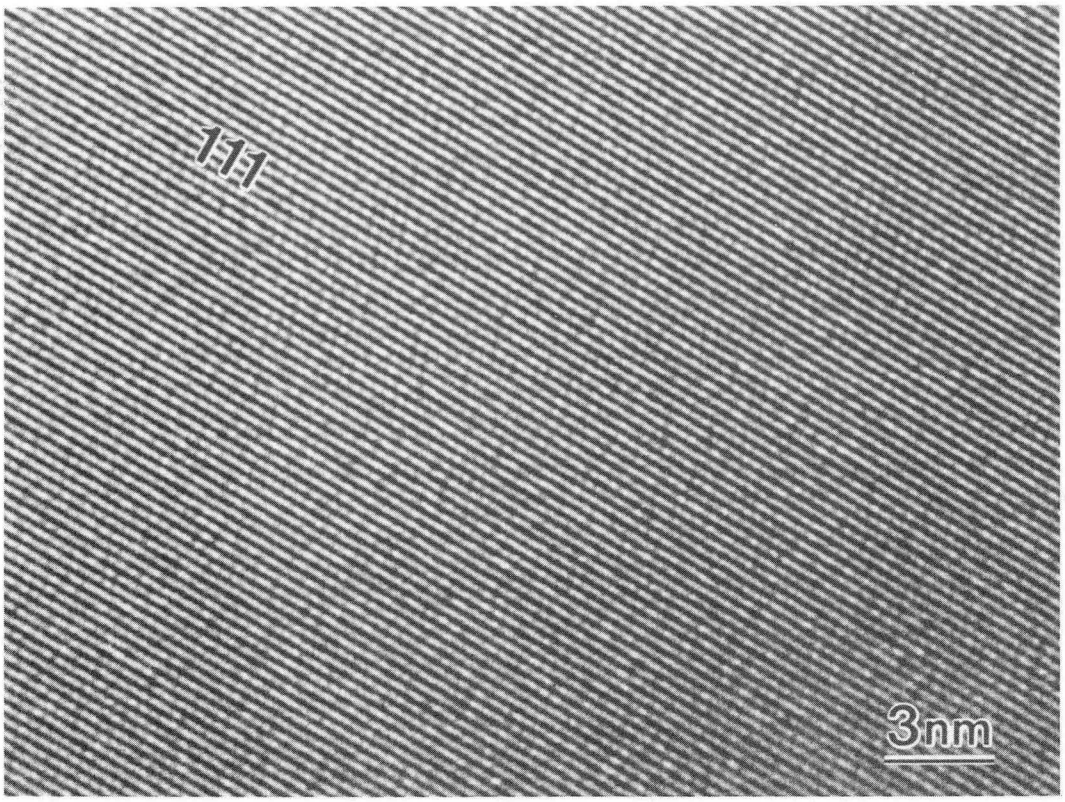

Fig. 5a

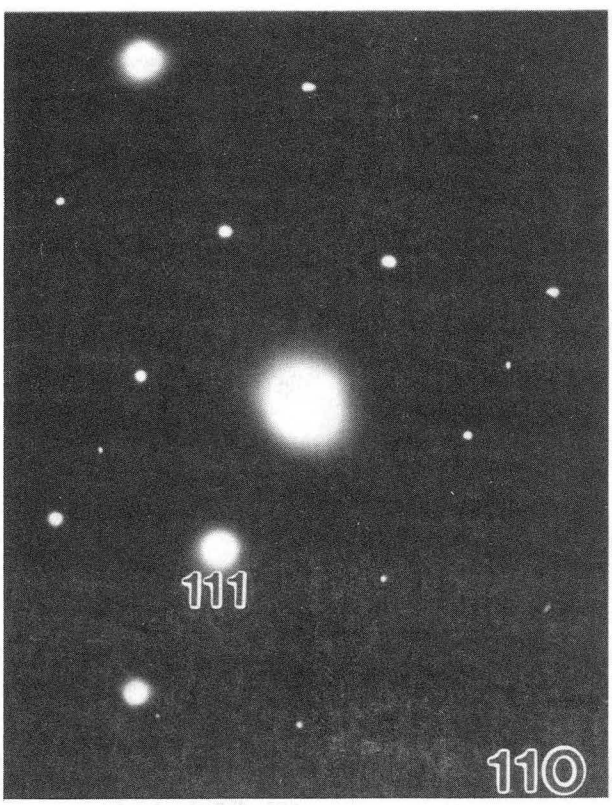

Fig. 5b

XBB-898-7091

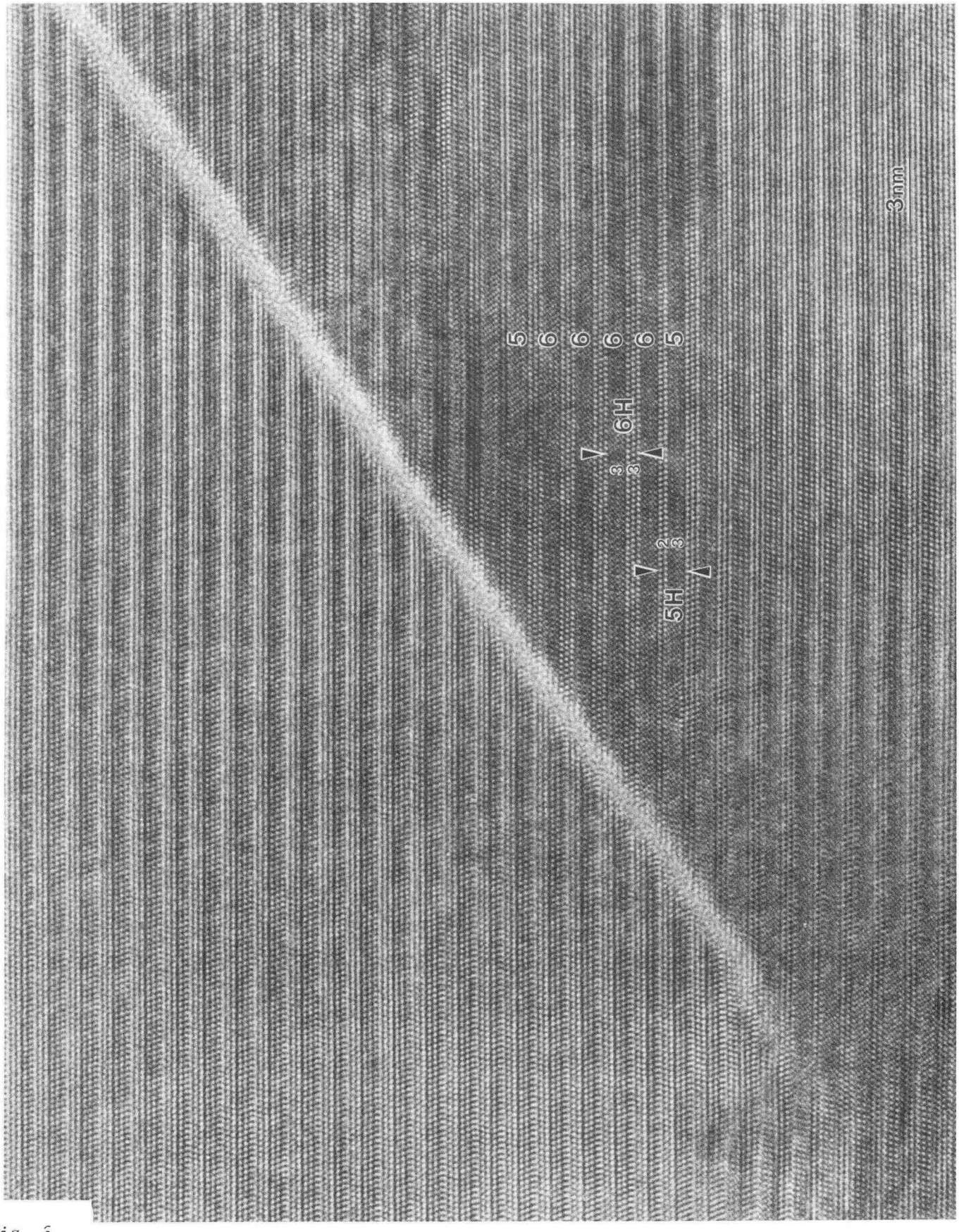

Fig. 6

XBB 898-7107

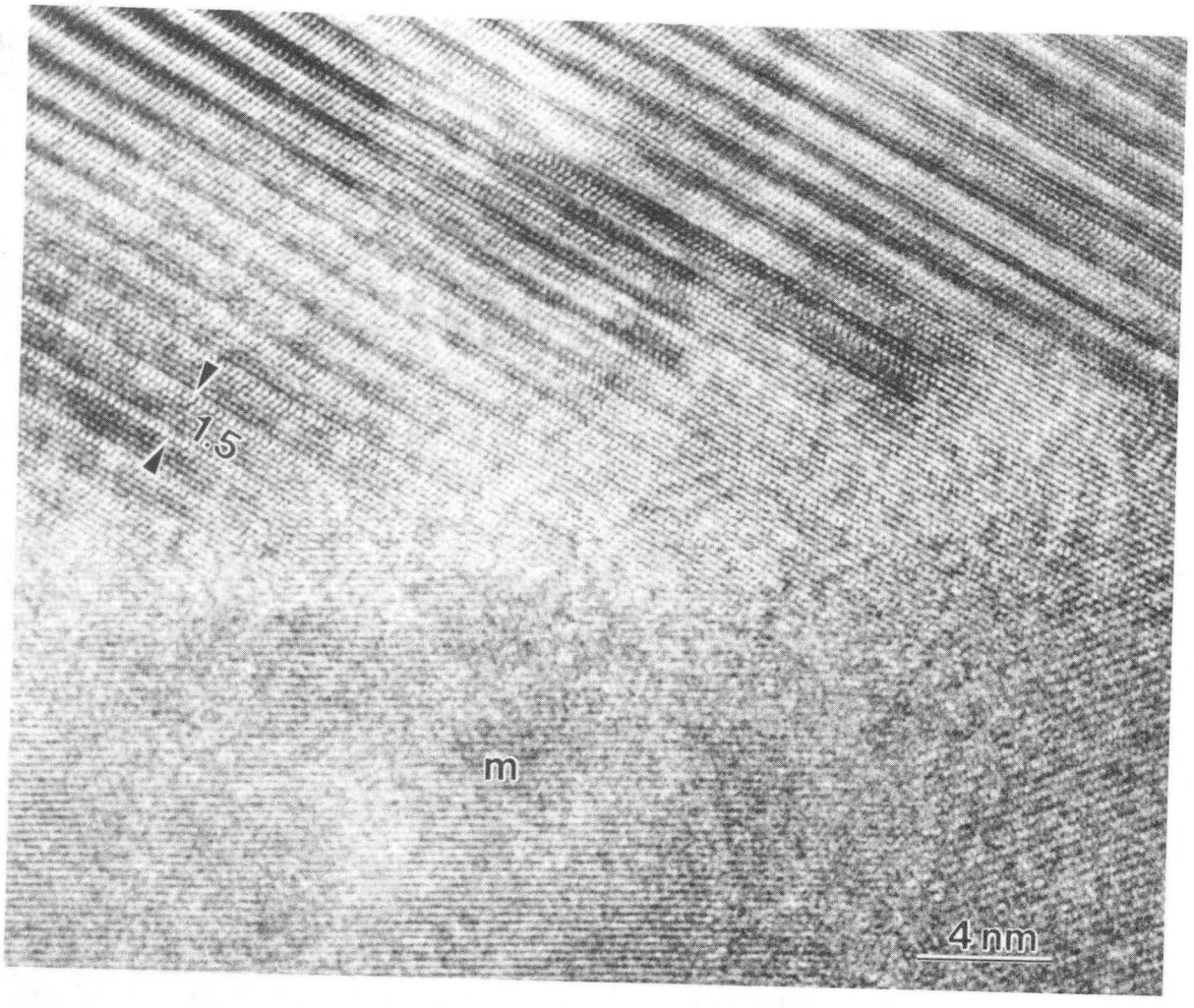

Fig. 7a

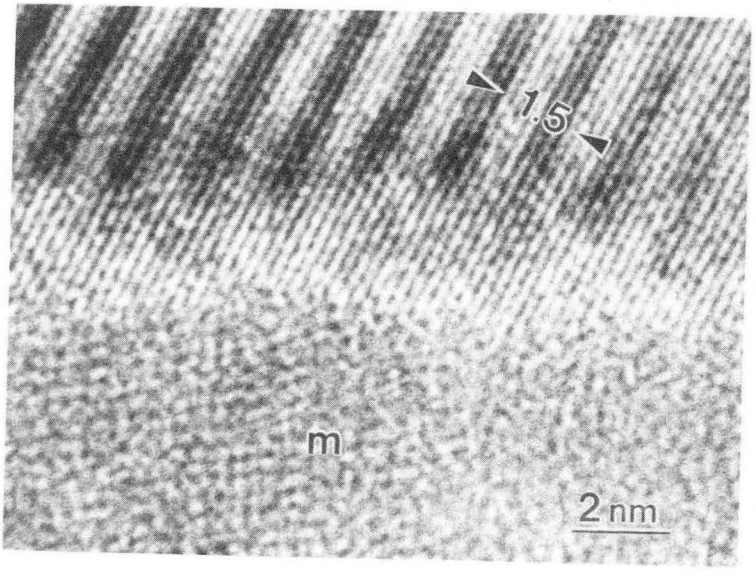

Fig. 7b

XBB 898-7093

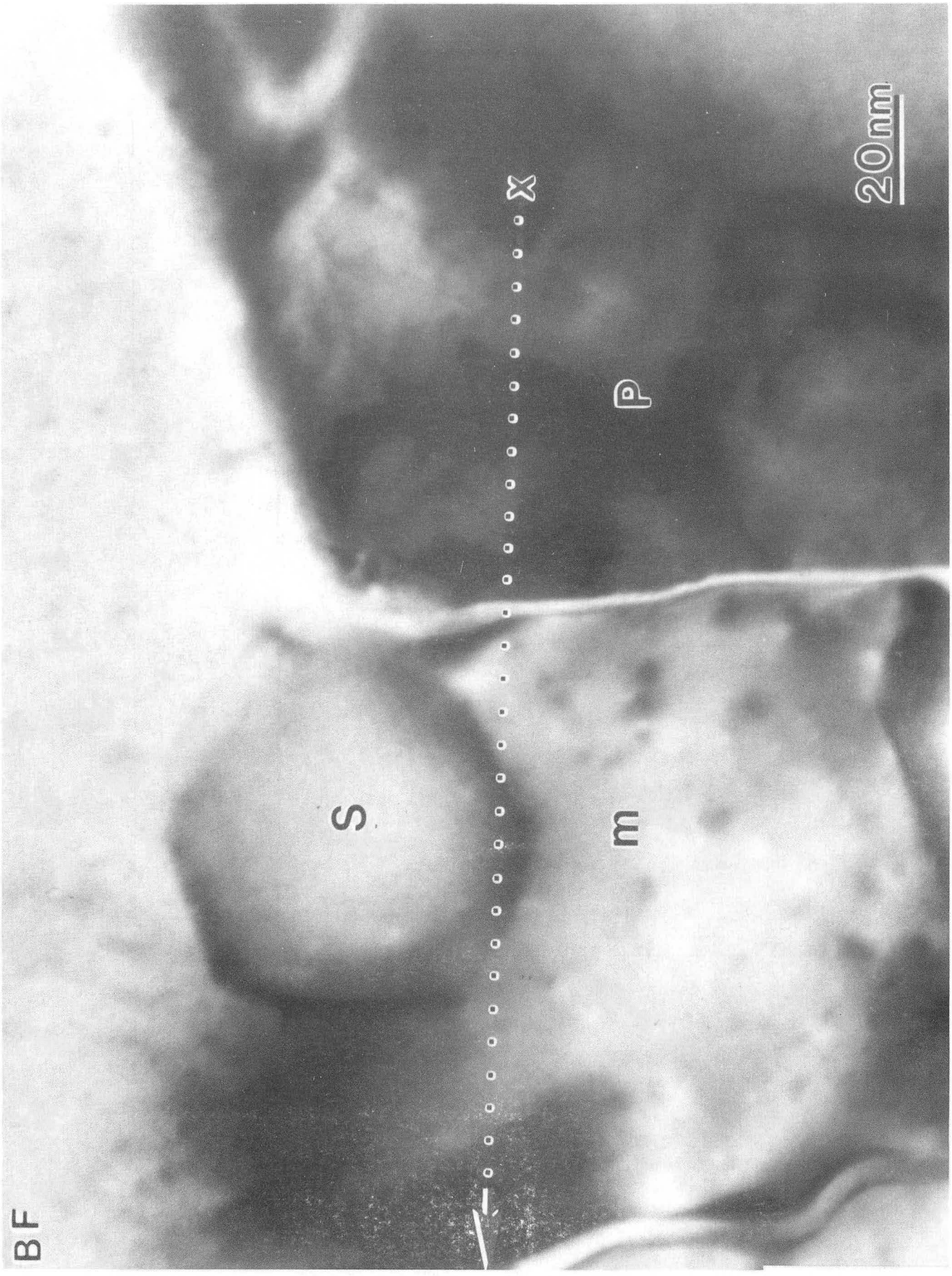

Fig. 8a

XBB 898 7100

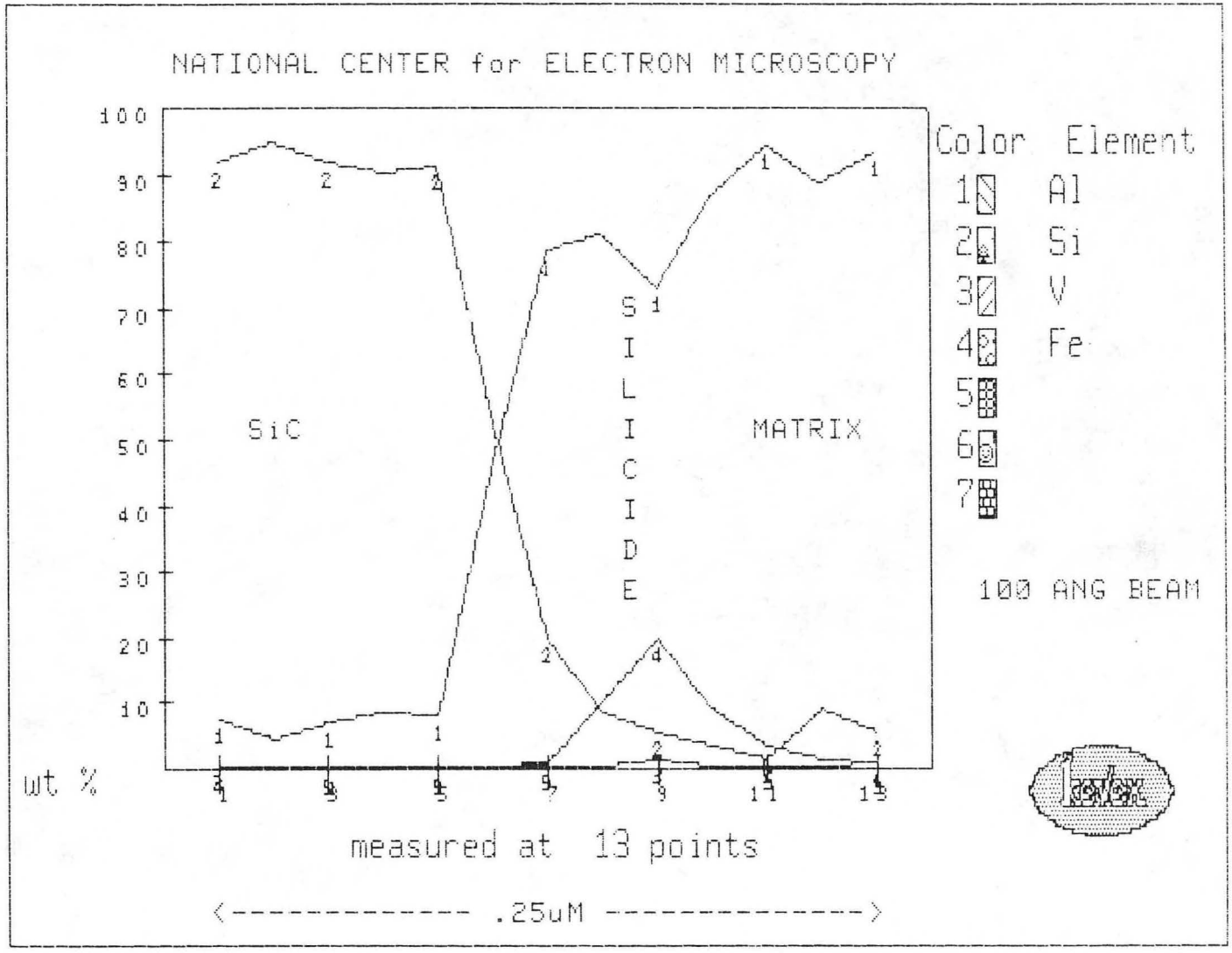
NATIONAL CENTER for ELECTRON MICROSCOPY
100
90
80
70
60
50
40
30
20
10
wt %
SiC
SILICIDE
MATRIX
Color Element
1 Al
2 Si
3 V
4 Fe
5
6
7
100 ANG BEAM
measured at 13 points
<---------- .25uM ---------->
leica

XBL 898-3134

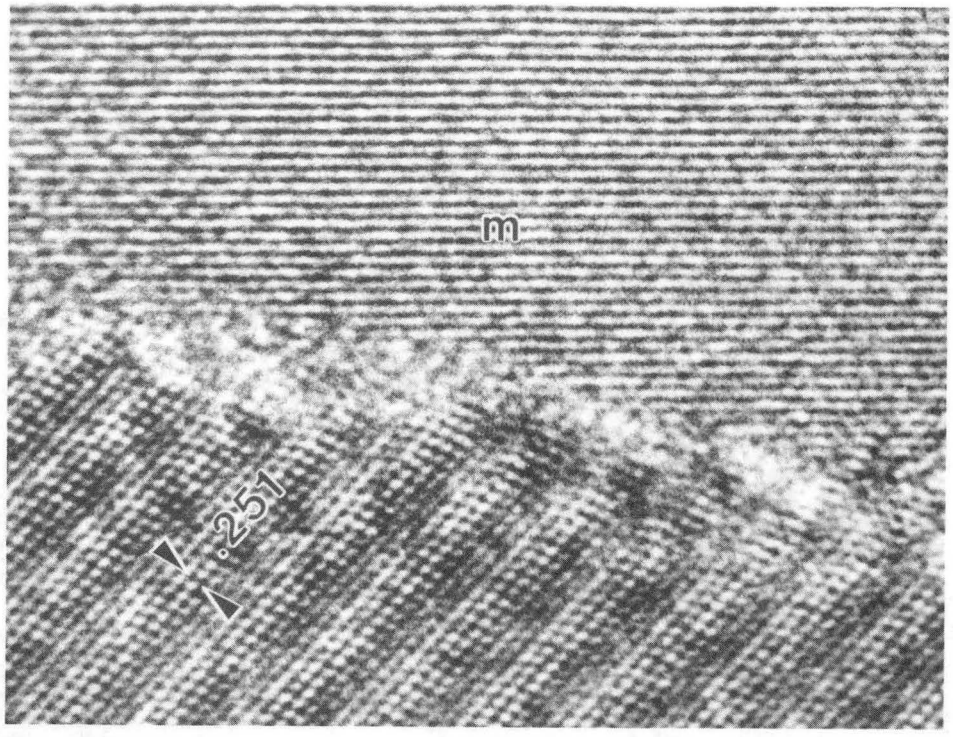

Fig. 9a

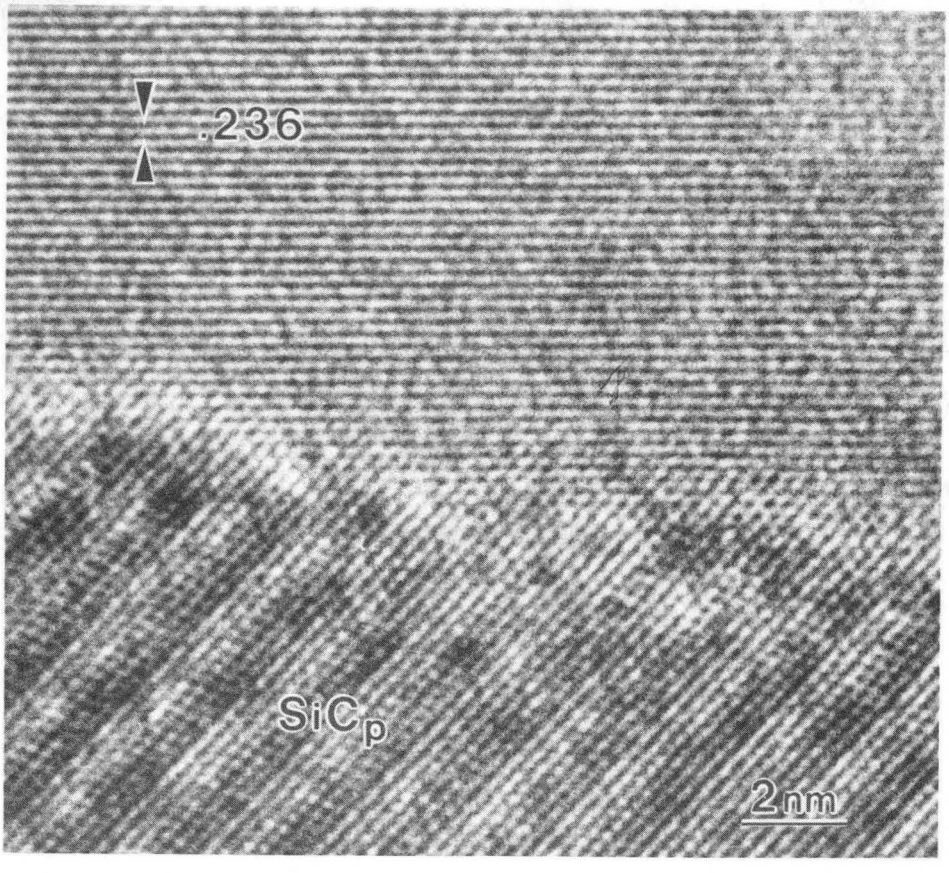

Fig. 9b

XBB 898 7099

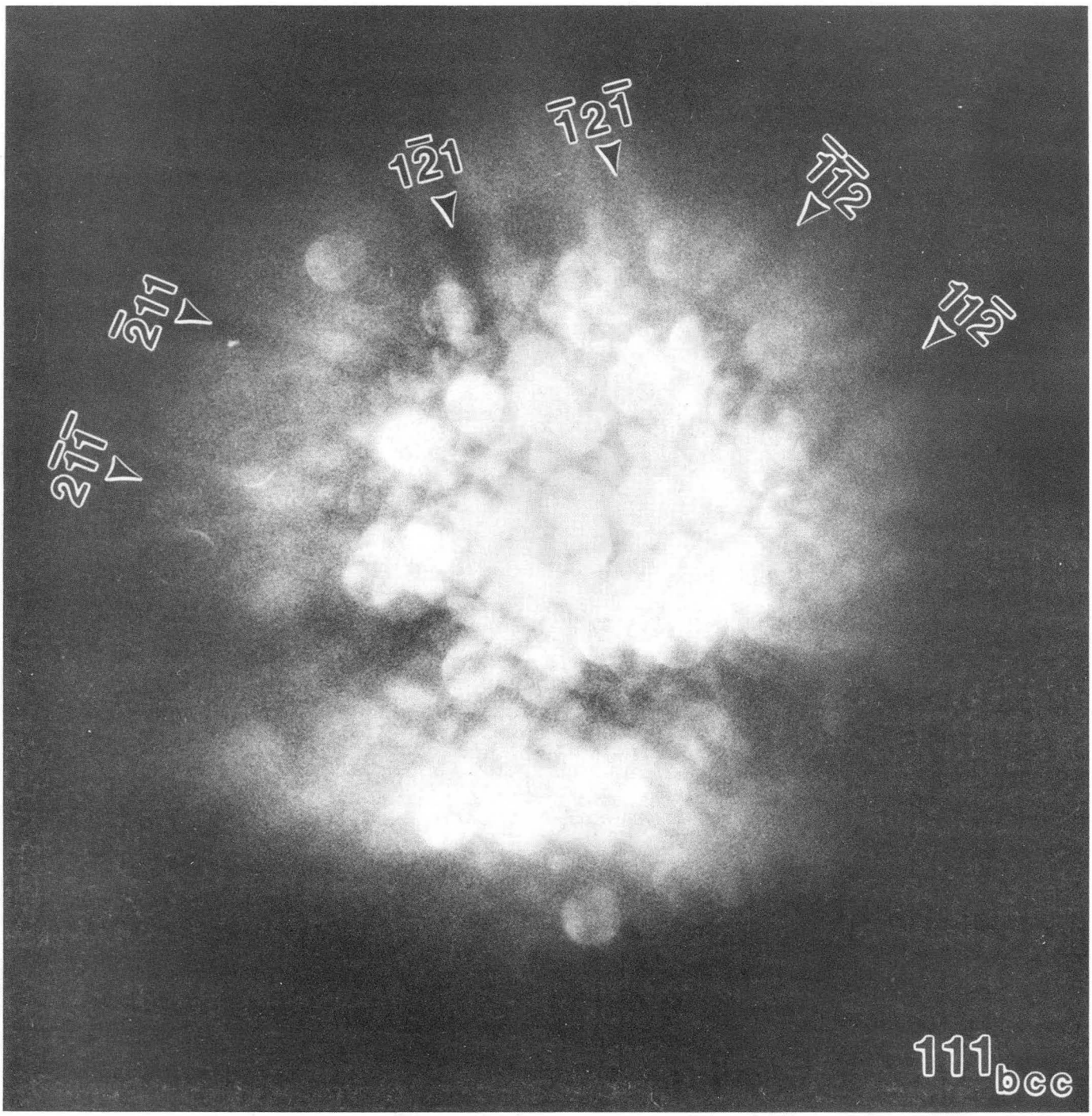

Fig. 10

XBB 898 7094

LAWRENCE BERKELEY LABORATORY
TECHNICAL INFORMATION DEPARTMENT
1 CYCLOTRON ROAD
BERKELEY, CALIFORNIA 94720